

## **Chitosan-Silver Nanocomposites: New Functional Biomaterial for Healthcare Applications**

Ramasubba Reddy Palem<sup>1</sup>, Nabanita Saha<sup>1</sup>, Ganesh D. Shimoga<sup>1</sup>, Zuzana Kronekova<sup>2</sup>,  
Monika Sláviková<sup>3</sup>, Petr Saha<sup>1</sup>

<sup>1</sup>Centre of Polymer Systems, University Institute, Tomas Bata University in Zlin, Zlin ,  
Czech Republic

<sup>2</sup>Department for Biomaterials Research, Polymer Institute, Slovak Academy of Sciences,  
Bratislava, Slovakia.

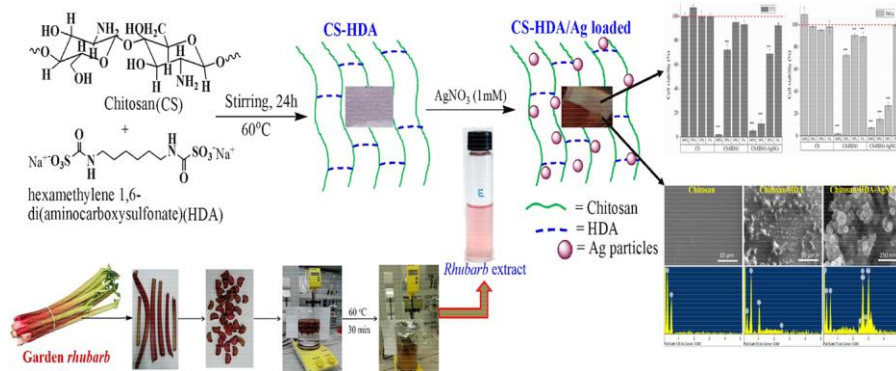
<sup>3</sup>Institute of Virology, Biomedical Centre, Slovak Academy of Sciences, Bratislava,  
Slovakia.

Corresponding Author: Nabanita Saha; nabanita@cps.utb.cz

### **Abstract**

Chitosan-Silver nanocomposites (CS-HDA-AgNCs) was prepared using chitosan (CS), biogenic silver nanocomposites (AgNCs) and cross-linker, hexamethylene 1, 6-di (amino carboxysulfonate) (HDA). The film is flexible and transparent. Its physical, mechanical, thermal, hydrophilicity and swelling properties were improved by HDA (2.5%). The antimicrobial activity of CS-HDA-AgNCs were not displayed any remarkable zone of inhibition but shows toxic effect in presence of normal 3T3 fibroblasts and cancer HeLa cells. It decreases to ca. 5 - 7 % for both cell lines. In conclusion, it can be mentioned that the CS-HDA-AgNCs, a kind of new functional biomaterial which could be useful for healthcare applications.

## Graphical Abstract



**KEYWORDS:** Chitosan, Green synthesis, Silver nanocomposites, Cytotoxicity, Anticancer activity

## 1. INTRODUCTION

Bio-based polymeric composites are the subject of interest of many Scientific and Research projects, as well as many commercial programs. Growing global, environmental and social concern, as well as new environmental regulations forced to quest for new bio-composites and green materials which could be compatible with the environment. Following the application of nanotechnology concept, it is achievable to create new biomaterials which provide new solutions mainly due to the small dimensions of the created systems. One of the most effective and promising biomaterials are nanocomposites based on silver nanoparticles and chitosan [1]. Chitosan is a natural second most abundant mucopolysaccharide available in the nature after cellulose. Its chemical structure consisting of  $\beta$ -(1-4)-linked D-glucosamine (deacetylated unit) and N-acetyl-D-glucosamine (acetylated unit) [2–5]. Due to unique properties such as nontoxic, chelating agent, mucoadhesive, biodegradable, biocompatible, bioabsorbable also possess gel forming ability [5], chitosan found many commercial applications. The polymer and

its derivatives are used as biomaterials in pharmaceuticals, cosmetics, medicine, implants, drug delivery, scaffold for tissue engineering, skin substitutes, wound dressings as well as in food industries [2, 5–6]. On the other hand, silver-nanoparticles are reported as most effective antimicrobial agents in a number of fields, such as medical and pharmaceutical, dental, coating and paint, membrane and food packaging purposes and life science (food, beverage storage applications and home appliances to water treatment) [1,6–15]. Therefore, effort has been given for the preparation of a novel functional biomaterial consisted with natural components like; Chitosan and plant mediated silver-nanoparticles (AgNPs) (prepared through green chemistry using garden *Rhubarb* stem extract acts as a reducing agent) [13, 16] where, HDA (hexamethylene 1,6-di (amino carboxysulfonate)) is used as a crosslinking agent [3–4, 17–18], which is stable in acidic aqueous solutions and readily reacts with amines [19]. Moreover, stability in the presence of amines and consequent long-term storage may be increased by the choice of an aliphatic diisocyanate, rather than a more reactive aromatic one [4]. Chitosan contains amino groups which are capable of binding silver and hence, silver release depends also on the chemical interactions between silver ions and chitosan. Moreover, both releases depend on the mass transport resistance caused by chitosan films.

The objective of present article is to report about chitosan-silver nanocomposites film; a novel functional biomaterials; could be beneficial for living beings. Hence, at first, hexamethylene 1,6-di(amino carboxysulfonate) (HDA), was prepared and cross-linked with CS film under heating condition. This crosslinked CS film termed as CS-HDA. Using this CS-HDA film as a template, chitosan based silver nanocomposites CS-HDA-

AgNCs films were prepared. Finally, the physical-chemical properties such as structural interactions, morphology, mechanical, thermal, wettability, swelling and crystalline nature of CS, CS-HDA and CS-HDA-AgNCs were determined. In order to observe the functional properties of the above mentioned biomaterials; cytotoxicity was performed in presence of 3T3 fibroblast cells and cancer HeLa cell using extracts of such films and direct contact incubation. The effects of CS, CS-HDA and CS-HDA-AgNCs on cell viability and cell morphology were examined.

## 2. EXPERIMENTAL

### 2.1. Materials

Chitosan (CS) (Deacetylation  $\geq 75.0\%$ ), hexamethylene 1,6 diisocyanate, silver nitrate ( $\text{AgNO}_3$ ), sodium hydroxide, was purchased from Sigma-Aldrich chemical Co., USA and used without any pretreatment. Other chemicals such as acetic acid, acetone, and sodium metabisulfite (analytical grade) were obtained from lach-ner (Czech Republic).

Nutrient agar was obtained from Hi-Media Chemicals. Normal 3T3-fibroblasts obtained from DSZ, Braunschweig, Germany, cancer Hela, cervix carcinoma obtained from the collection in the Institute of virology BMC SAV, Bratislava, Slovakia. Dulbecco's Modified Eagle Medium (DMEM), fetal bovine serum (FBS), streptomycin, penicillin, Trypsin-EDTA and L-glutamine were purchased from Gibco (Life Technologies, Grand Island, NY, USA). Dimethyl sulfoxide (DMSO) was purchased from Sigma-Aldrich (Weinheim, Germany) and 3-(4,5-Dimethyl-diazol-2-yl)-2,5-diphenyltetrazolium bromide (MTT) was purchased from Calbiochem (Merck Millipore, Darmstadt, Germany). All

other chemicals are analytical grade and used without further purification, deionized water was used throughout the experiments.

## **2.2. Preparation Of Pure And Crosslinked Chitosan Films**

Chitosan (CS) films were prepared by the dissolution of 4 g of chitosan in 400mL of acetic acid (2%) solution. To achieve the cross-linked chitosan film (CS-HDA), the cross-linker hexamethylene 1,6-di (amino carboxysulfonate) (HDA) was synthesized freshly following the protocol [4] obtained white powder form of HDA. Different amount (2.5, 5.0 and 7.5 weight %) of HDA (see Table.1) was added to the polymer solution of chitosan. These three different polymer (CS-HDA) solutions were stirred overnight at 60°C temperature and allowed to form the films via the solution casting method using glass petri plates (18mm diameter). The dried CS-HDA film was dipped in distilled water for 24 h to remove any unreacted impurities and then kept for drying at room temperature. The dried films were used for the preparation of chitosan based silver nanocomposites (CS-HDA-AgNCs) and further analysis.

## **2.3. Preparation Of Chitosan - Silver Nanocomposites**

Firstly, 200 mg of pure CS and CS-HDA films were individually immersed in 30 ml of 1mM AgNO<sub>3</sub> solution at 25°C for 12 h. After that the remaining solution discarded and were added freshly prepared aqueous *rhubarb* stem extract (20 ml) into the silver embedded chitosan films (CS and CS-HDA). The addition of *rhubarb* extract (pink color) to AgNO<sub>3</sub> solution (colorless) led to turning the solution color into ruby red, indicating the formation of silver nanoparticles. The silver salts presented in chitosan based films

were reduced by functional moieties such as physcion, emodin, aloemodin, and rhein are present in the *rhubarb* extract involved in the reduction and stabilization of AgNCs [13]. The pictorial representation of synthesis of chitosan silver nanocomposites are depicted in Scheme 1. These silver nanocomposites films of CS and CS-HDA are designated as CS-AgNCs and CS-HDA-AgNCs respectively.

#### 2.4. SWELLING STUDIES

In order to investigate the swelling behavior of chitosan based films various amounts (2.5, 5.0 and 7.5 weight %) of HDA were conducted using a conventional gravimetric method [4]. The films were kept in a vacuum desiccator for 24 h before determining the dry weight ( $W_d$ ) by weighing to  $\pm 0.0001$  g places on an electronic balance. The chitosan based films were immersed in deionized water at 25°C for 24 h. The excesses of water was wiped with filter paper and then weighed to determine swollen weight ( $W_s$ ). The equilibrium swelling ratio (ESR) values are depicted in Table.1, calculated by following Eqn. (1).

$$\text{ESR \%} = \left( \frac{W_s - W_d}{W_d} \right) \times 100 \quad (1)$$

#### 2.5. Characterization

The UV-Vis spectroscopic measurements were carried out using VARIAN-EL08043361 spectrometer from 200 to 600 nm at room temperature. The FTIR spectra of the films were recorded with a FTIR spectrophotometer (Thermo Scientific iS5, iD5 ATR) in the scanning range from 4000-600  $\text{cm}^{-1}$ , at a scan rate of 64  $\text{cm s}^{-1}$  and measuring with Ge crystal with 4  $\text{cm}^{-1}$  resolution. The thermal stability of films was measured by

thermogravimetric analysis (TGA) using a thermal analyzer TGA Q500 (TA instruments, USA). The weight loss of material was determined at 10°C/min heating rate between temperature ranges from 25 to 600°C under nitrogen atmosphere (flow rate 50ml/min, initial sample weights were about 12±0.9mg). X-ray diffraction (XRD) patterns of the films were recorded on a PANalytical X'Pert PRO X-ray diffractometer using CuK $\alpha$  radiation ( $\lambda=1.5406 \text{ \AA}$ ) at a step size 0.02°, speed 10°/min and operating at 40 kV and 15 Ma, in the scanned range from 5 to 90°. The morphology of films was recorded using a Scanning electron microscope (Nova NanoSEM450, FEI), at an acceleration voltage of 5-15 kV. The size and morphology of AgNCs were recorded on Transmission electron microscope (TEM, Technai F20); operating at an accelerating voltage of 200 kV. For this measurement, the colloidal Ag solution (10-20  $\mu$ l) was extracted from CS-AgNCs and CS-HDA-AgNCs placed on a copper grid and dried prior to measurement for 2-3h at 60°C.

## **2.6. Contact Angle Measurement**

Contact angle measurement is one of the common method to evaluate the surface wettability of any film. Pure CS is soluble in acidic aqueous condition, but the cross linked CS (i.e. CS-HDA) is not soluble but swelled. Wound dressing application point of view, hydrophobicity nature of film is one of the important properties; that should not easily soluble in the aqueous medium. The contact angle of water on the film surface was determined using contact angle measurement device (Advex Instruments, Czech Republic). The contact angle was measured exactly 30 seconds, just after a water droplet was dropped on the film surface (CS, CS-HDA & CS-HDA-AgNCs) at room

temperature. For each sample, five measurements were performed at different locations on the film.

### **2.7. Mechanical Measurements**

The mechanical properties of the CS and CS-HDA films were measured by using a tensile testing machine (Testometric MT350-5CT). Each sample was kept in an incubator with 58% humidity at 25°C for 48 h. These films were cut into 10 mm width and 40 mm length. The strips were then placed between pneumatic clamps separated at a distance of 25 mm and running at a cross head speed of 20 mm/min. The tensile strength, elongation at break and young's modulus was measured using a 500 kg load cell. For each sample, five uniformly thick strips were tested and mean value of tensile strength, young modulus, elongation at break were reported [17].

### **2.8. Antimicrobial Activity**

The antimicrobial activity of pure CS, CS-HDA, and CS-HDA-AgNCs films verified by the disc diffusion method using two bacteria (*E. coli* and *S. aureus*) and two fungi (*A. niger* and *C. albicans*) were chosen as a model. The nutrient agar (NA) for bacteria and Sabouraud's dextrose medium (SDM) for fungi was prepared. The sterilization of nutrient media (NA and SDM) was done in 250ml sealed bottle at 120°C for 20 min at a pressure of 15lb, then poured separately into sterilized petri dishes. After solidification of the media, 1ml of bacterial suspension were flooded uniformly. The film discs (8 mm diameter) were placed on the surface and incubated for 24 h at 37°C in a temperature



controlled incubation chamber. After 24 h, the least effect inhibition zones were identified surrounding the films. Each assay was performed in triplicate.

## 2.9. Cell Viability Assay

Cells were grown in full growth medium (DMEM, 10% FBS, Penicillin-Streptomycin) at 37°C in a CO<sub>2</sub> incubator with 5% CO<sub>2</sub> and saturated humidity. For cytotoxicity (direct contact) test, cells at concentration 100000 cells per well, were seeded in 24 tissue culture plate and incubated overnight. Next day, the film (5mm diameter, thickness <0.5 mm) of CS, CS-HDA and CS-HDA-AgNCs were placed into wells in quadruplicates (n=4) and then incubated for 24 h. After 24 h, the cell morphology around the films was documented, films were removed and MTT assay was performed. For cytotoxicity (using extract) test, cells at concentration 5000 cells per well, were seeded in 96 tissue culture plate and incubated overnight. Before collection of extraction, the films (CS, CS-HDA and CS-HDA-AgNCs) were rinsed with phosphate buffer solution (PBS) for 1 minute and then put into the full growth medium (6 cm<sup>2</sup>/ml) according to ISO 10993-12 and incubated 24 h at 37°C in the sealed tube. After 24 h extraction, the full extract and their dilutions (1:10, 1:50 and 1:100) were put into the cells in the 96 well plates for 24 h treatment. Cell viability was estimated via MTT assay.

**MTT assay:** after the incubation, medium was replaced with medium containing MTT at concentration 0.5 mg/ml and incubated for 2 h. Afterwards MTT medium was removed and DMSO was added. The absorbance was measured by plate reader at the wavelength 595 nm.

## STATISTICAL ANALYSIS

All results are presented as mean  $\pm$  standard deviation (SD) from quadruplicates (n=4). Statistical analysis was performed using the one way ANOVA test followed subsequently by means comparison with Turkey test.

## 3. RESULTS AND DISCUSSION

In the present study, homogeneous and flexible chitosan based films were obtained by solution casting after drying at room temperature. Visually, pure CS and CS-HDA films are transparent. The fabrication of plant mediated AgNCs involves the following steps: the preparation of chitosan films with sequential cross-linking followed by the reduction of silver ions with aqueous *rhubarb* stem extract. The versatile advantages of this new material are simple method in preparation, inexpensive, improved mechanical, thermal and swelling properties and having biocompatible nature. The complete protocol adopted for green approach of chitosan AgNCs is illustrated in Scheme 1.

### 3.1. Optical And UV-Vis Analysis

As it can be seen from Fig. 1A, initially the pure CS and CS-HDA film was homogeneous and transparent. After treatment with AgNO<sub>3</sub>, the films become pale yellow. All films first dipped in 30 ml of 1mM AgNO<sub>3</sub> solution for 12 h, then freshly prepared *rhubarb* extract was added then started the formation of Ag particles and traced by UV-Vis spectroscopy according to the characteristic silver surface plasmon resonance (SPR) band is observed at 433 nm as shown in Fig. 1B, indicates the formation of nano

sized silver nanoparticles. According to Rao et al. the SPR band for polymeric silver nanoparticles was observed in the range between 380 to 450nm [20]. Moreover, these silver nanoparticles were uniformly dispersed in the network of CS-HDA-AgNCs film. This is due to *rhubarb* extract which acts as capping agent and also captured by the network through functional groups (i.e.  $-\text{NH}_2$ ,  $-\text{OH}$ ). However, after formation of silver nanoparticles these films were changed into ruby red color, the color of the films did not change on storage for several months indicating stability of AgNCs.

### 3.2. FTIR Spectroscopy Analysis

The FTIR spectra of CS, CS-HDA (2.5%, 5.0% and 7.5%) and CS-HDA-AgNCs films are depicted in Fig. 2. The pure chitosan film exhibits characteristic broad band around  $3636\text{--}3106\text{ cm}^{-1}$  due to the stretching vibrations of overlapped primary amine ( $-\text{NH}_2$ ) and hydroxyl groups ( $-\text{OH}$ ), the bands at  $2913\text{ cm}^{-1}$  and  $2847\text{ cm}^{-1}$  due to aliphatic C–H stretching and  $-\text{NH}_2$  bending vibrations, the bands at  $1655\text{ cm}^{-1}$  and  $1564\text{ cm}^{-1}$  corresponding to C=O stretching vibration (Amide I) and N–H angular deformation (Amide II), bands at  $1410\text{ cm}^{-1}$  for  $-\text{CH}_3$  symmetrical angular deformation,  $1377\text{ cm}^{-1}$  for C–O stretching mode of  $-\text{CH}_2\text{--OH}$  group, band at  $1319\text{ cm}^{-1}$  for C–N amino group axial deformation. However, several absorption bands at 1158, 1076, 1038, 938, 895, and  $759\text{ cm}^{-1}$  are due to C–O and C–N stretching vibrations, C–O–C stretching vibrations from  $\beta$ -glycosidic bond and N–H wagging of the saccharide structure of chitosan. In comparison to the spectra of pure chitosan, except for the same peaks from the characteristic bands of saccharide structure, the spectra of CS-HDA1 showed a sharp absorption peak at 1747,  $1150\text{ cm}^{-1}$  due to C=O stretching (urea), C–N stretching increases and loss of peaks at

1158, 1076, 1038 was observed for the cross-linker 2.5%. The cross-linker 5.0%, 7.5% in CS-HDA2 and CS-HDA3 showed a sharp peak at  $3335\text{ cm}^{-1}$  indicating the increased presence of N–H and decreased presence of  $\text{–NH}_2$ . The carbonyl peak shifted from an amide I band at  $1655\text{ cm}^{-1}$  to  $1680\text{ cm}^{-1}$  due to urea containing  $\text{–C=O}$  bond in cross-linker. The band at  $1537\text{ cm}^{-1}$  due to the presence of a urea bond, it is formed when HDA reacts with a free amine group. Also formation of new peaks at 1247, 1216, 1125, 1049  $\text{cm}^{-1}$  was observed for crosslinking above 2.5%. After cross-linking concentration increases, a new band was observed in CS-HDA1, CS-HDA2 and CS-HDA3 at  $727\text{ cm}^{-1}$  is a strong indication of a  $\text{–CH}_2$  group in cross-linker. From the above results it confirms chitosan crosslinked with HDA.

The FTIR spectra of the prepared CS-AgNCs and CS-HDA-AgNCs were compared with CS and CS-HDA films. The spectrum of AgNCs showed bands at  $2913\text{ cm}^{-1}$  (C–H stretching),  $1410\text{ cm}^{-1}$  ( $\text{–CH}_3$  bending) these bands are not sensitive to metal nanoparticle surface. The interactions of amine, hydroxyl bands as well as amine bending vibrations ( $1556\text{ cm}^{-1}$ ) in CS and CS-HDA groups slightly shift to lower wave number and decrease in intensity due to coordination between silver nanoparticles and N–H/O–H groups. From the above results, the FT-IR spectrum supports the CS cross-linked with HDA and presence of silver nanoparticles in the CS and CS-HDA films.

### **3.3. SEM And EDS Analysis**

The surface morphology, size and elemental composition of pure CS, CS-HDA and green synthesized CS-HDA-AgNCs was analyzed using SEM and EDS, images are depicted in Fig. 3.

Here, reported about the film CS-HDA which is prepared with 2.5% cross linker and denoted as CS-HDA1. The pure CS film displayed smooth and homogeneous surface, whereas the CS-HDA1 showed a rough surface along with some granules. This is due to the excess of HDA which did not attend the crosslinking reaction with chitosan and remained on the surface during the drying process. The biosynthesized CS-HDA1-AgNCs are homogeneous and relatively spherical in shape. Next, the corresponding EDS spectrum provides quantitative and qualitative status of CS, CS-HDA1 and Ag nanoparticles in CS-HDA1-AgNCs. The pure CS confirms presence of carbon (with high intensity) and oxygen elements only, while in the case of CS-HDA1 shows carbon and oxygen (with high intensity) elements along some impurities this confirms HDA undergoes crosslinking with chitosan. Finally, the CS-HDA1-AgNCs film revealed a strong elemental peak at around 2.5–3.0 keV which is in congruence with the major emission peaks specified for silver (metallic), which confirmed uniform dispersion of elemental Ag in the CS-HDA1 network. This result is consistent with the literature values Reddy et al. [13]. Along with this, carbon, oxygen and chlorine elements also observed because the silver nanoparticles capping with bio-molecules of *rhubarb* extract. Apart from these peaks, Sulphur element peak was observed. This indicates the formation of some impurities along with silver nanoparticles.

### 3.4. TEM Analysis

The size, shape and morphology of the green synthesized CS-HDA-AgNCs are shown in Fig. 4. In Fig. 4a, the low magnification TEM image indicates that the morphology of the silver particles is spherical in shape and also observed small with a narrow size distribution from several nm to 50 nm. Also observed that the silver nanoparticles formed along with the polymer chains and Ag entrapment in the CS-HDA networks. Two different shaped silver nanoparticles (green synthesized or plant mediated) were noticed relatively bigger one and the ultra-small one (Indicated by yellow arrow mark). The high magnification TEM image is shown in Fig. 4b around 2 nm. From the above results, it is clearly indicated that Ag nanoparticles deposited on chitosan based network and the average particle size of Ag nanoparticle lies between 2-50 nm.

### 3.5. Thermal Analysis

To gain a better understanding of the thermal decomposition properties of the pristine CS, CS-HDA1 and their silver nanocomposites were studied with a thermogravimetric analysis. The thermal decomposition of pristine CS (a), CS-HDA1 (b), and their AgNCs (c, d) was studied using TGA and dramatically carried out between weight loss (%) versus temperatures is given in Fig. 5. The first step involves in all compositions around 60-150° (the line indicated by orange arrow) a smaller weight loss (8-10%) due to the initial loss of moisture vaporization (water molecules) and some impurities were observed in all compositions. The second step starts around 230° (the line indicated by orange arrow) and continued up to 500°, the maximum decomposition was observed for

CS, CS-HDA1, CS-AgNCs and CS-HDA1-AgNCs at 278°, 283°, 281° and 295° respectively. The CS-HDA1 shows a total weight loss (51%) as compared to pristine CS (54%) indicating, the crosslinking decreases the rate of degradation and increases the stability. The CS-AgNCs decomposition showed less weight loss (53%) as compared to pure CS. Similarly the CS-HDA1-AgNCs decomposition showed less weight loss (48%) as compared to CS-HDA1 (51%). From the above results, the CS-HDA shows thermally more stable than pristine CS similarly, the CS-HDA1-AgNCs shows more stable than CS, CS-HDA1, and CS-AgNCs respectively.

### 3.6. X-Ray Diffraction Analysis

The XRD patterns of pure CS, CS-HDA1, and CS-HDA1-AgNCs films are shown in Fig. 6. The pure CS exhibit diffraction peaks at  $2\theta$  of 9.8 and 15.0° (Fig. 6a) corresponding to anhydrous and hydrated chitosan crystals, an additional broad peak was observed at 20.9° corresponding to (110) planes, which corresponds to the characteristic peak for chitosan films. The CS-HDA1 film shows sharpening and additional diffraction peaks at 11.5, 15.5, 18, 20, 22.8, 25, 29, 32, 34, 37.5, 42, and 52° (Fig. 6b). The crosslinked chitosan shows a sharp peak at 32° corresponding to (200) crystalline plane which corresponds crystalline nature.

The crosslinked chitosan films was embedded with silver nanoparticles by bio-reduction processes with *rhubarb* stem extract in Fig. 6c. The diffraction peaks at  $2\theta$  value of 28, 32.5, 46.5, 55.3, 58, 67.7, 76.7 and 85.8 corresponding to (111), (200), (220), (311),

(400), (420), and (422) crystalline planes were observed. This confirms presence of silver nanoparticles with face centered cubic structure having crystalline nature.

### **3.7. Swelling Properties**

The equilibrium swelling study of the CS-HDA film containing 0.0%, 2.5%, 5.0% and 7.5% of HDA were performed at 25°C in deionized water. It provides an extent of cross-linking in the polymer network, where higher crosslink (7.5%) densities correspond to decrease swelling ratio (36.52%) as shown in Table.1. The pure chitosan doesn't show swelling because it is soluble in water, after cross-linking the CS-HDA shows swelling property, this is due to HDA makes irreversible chemical links between the polymer strands so that these linkages allow the polymer network to be exposed to water. These films swollen to equilibrium in deionized water showed a steady decrease in equilibrium water content with increasing HDA cross-linker, indicating increased cross-link density. The cross-linking changes not only the density of the CS-HDA film as observed from the XRD data, but also the chemical nature of the CS-HDA film such as hydrophilicity. The swelling property of chitosan based films is useful in charge/discharge process in supercapacitor [21], moisture food packaging [22] and wound dressing [23] applications.

### **3.8. Mechanical Properties**

Mechanical properties play a vital role in the design of biomaterials for medical applications. Tensile strength of any material taken in an account for how much stress the material will bare before suffering permanent deformation or tearing. As we know that pure chitosan is aqueous soluble, brittle and hydrophilic biopolymer due to this reason the



blocked diisocyanate (HDA) was used to cross-linkage and to avoid the solubility as well as to improve the tensile strength and flexibility. The tensile strength of chitosan films containing 0%, 2.5%, 5.0% and 7.5% of HDA are depicted in Table.1. It is seen that the extensibility of films reduced (lower elongation at break) as strength of films increased (greater tensile strength). The highest tensile strength observed for CS-HDA (2.5%) is 48.06 MPa, after cross-linking increases the tensile strength decreases. The lowest strength was observed for pure CS is 22.44 MPa. From the above results, the cross-linked films improved their tensile strength and Young's modulus values compared to pure chitosan film.

### 3.9. Contact Angle Measurement

The water contact angle and surface energy value measurements can reflect the wettability properties of the pure CS, CS-HDA1, and CS-HDA1-AgNCs films. The contact angle measurements were performed exactly 30 seconds after a water droplet was dropped on the pure CS, CS-HDA1, and CS-HDA1-AgNCs film surface and the reported values were averages of at least five measurements performed at different locations of the films. The contact angle values of these films are depicted in Fig. 7. It can be seen from the figure that the surface energy value is higher for CS-HDA1 ( $62.70 \text{ mJ/m}^2$ ) compared to pure CS ( $51.52 \text{ mJ/m}^2$ ), and CS-HDA1-AgNCs ( $60.53 \text{ mJ/m}^2$ ) respectively. The contact angle of CS-HDA1 ( $33.6^\circ$ ) film is less compared to pristine chitosan ( $34.5^\circ$ ) and CS-HDA1-AgNCs ( $37.8^\circ$ ) due to hydrophilic nature increases after cross-linking with HDA. However, the CS-HDA1-AgNCs film is less hydrophilic compared to CS-HDA1 due to Ag particles complexation with amide and hydroxyl groups.

### 3.10. Antimicrobial Activity

We investigated the antimicrobial activity of chitosan based films against bacteria and fungi by diffusion method. The moderate growth of inhibition was observed in the case of bacteria and fungi as shown in Fig. 8. Because after cross-linking the free amine groups are converted into covalent bonds, the lower molecular weight chitosan used as well as the degree of deacetylation is  $> 75\%$ . After silver loaded the extracted solution shows the biocompatible nature, so that in solid form the particles are not able to out from the surface due to this reason pure CS, CS-HDA and CS-HDA-AgNCs films does not involve much in the growth inhibition processes. According to Tripathi et al pure chitosan film didn't show any inhibitory property, but its chitosan based silver nanocomposites showed good inhibitory property against *E. coli* and *S. aureus*, used as food packaging material [24]. However, the bacterial concentration also may effects (1000 $\mu$ L/each plate) during inoculum, the bacterial growth was not observed.

### 3.11. In-Vitro Cytotoxicity Studies

Cytotoxicity of extracts of nanocomposite films was analyzed using normal 3T3 fibroblasts and cancer HeLa cells as shown in Fig. 9. Pure CS films extracts are not toxic to both cell lines after 24 h treatment. Full extracts (100%) obtained from CS-HDA1 films decrease cell viability to ca. 2 - 3 % for both cell lines, but after 50% dilution the cell viability increases to ca. 70 % and with higher dilutions the viability increases reasonably to untreated control cells. The low cytotoxicity of full CS-HDA1 extracts might be affected by slightly acidic pH. Viability of cells treated with full extracts

(100%) obtained from CS-HDA1-AgNCs films decreases to ca. 5 - 7 % for both cell lines and with dilutions the viability increases and only the highest dilution (1% extract) leads to cell viability compare to untreated control cells. As is seen from Fig. 10A where cytotoxicity of all extracts are compared between both cell lines, the cell viability after treatment with CS and CS-HDA1 extracts are similar with no significant differences. However, if cells are treated with extracts containing AgNCs significant difference is observed using 10% extracts, where normal 3T3 fibroblasts are less sensitive and cell viability is 70 % compared to cancer HeLa cells with viability around 30%. So this concentration of AgNCs in film extracts is cytotoxic to cancer HeLa cells, but biotolerable by normal cells. The effect of CS-HDA1-AgNCs films on cancer cells is also confirmed by direct contact cytotoxicity, where significant difference in cell viability is observed between the cell lines (see Fig. 10B).

However, the CS and CS-HDA1 films are not cytotoxic to the both types of cells, morphology of cells is not changed as seen in Fig. 11. Cells in direct contact and in close proximity to CS-HDA1-AgNCs films are dying due to nanoparticle release in the case of HeLa cells but in 3T3 fibroblasts. The morphology of cells is changed; cells are of more round shape. In addition, HeLa cells seem to be more sensitive as the HeLa cells are mostly of round shape or even cell debris (black spots) is observed, while with 3T3 fibroblasts also cells with normal morphology (without cell debris) are present.

From the above results, we suggest that the biologically synthesized silver nanocomposites may provide potent anticancer activity and also reduces the side effects on normal cells.

## 5. CONCLUSION

In precise, we prepared chitosan based novel functional biomaterial / films by simple solution casting approach using HDA cross-linker and their silver nanocomposites were synthesized by garden *rhubarb* extract without using external chemical-reducing agents. The size of nanocomposites is < 100 nm. These films are flexible and transparent, the physical, mechanical, thermal, hydrophilicity and swelling properties were improved by the crosslinking. The antimicrobial activity of chitosan based silver-nanocomposites were not displayed any remarkable zone of inhibition. Pure CS film extracts are not toxic for normal 3T3 fibroblasts and cancer HeLa cells. However, the CS-HDA1 films decrease cell viability to ca. 2-3 % for 100% extract, but with higher dilutions the viability increases moderately than untreated controlled cells. In the case of CS-HDA1-AgNCs films decreases to ca. 5 - 7 % for both cell lines and with dilutions the viability increases and only the highest dilution (1% extract) leads to cell viability in comparison to untreated control cells. Hence, based on the results, the bio-based polymer composites CS-HDA1-AgNCs films considered as one of the novel and promising biomaterial for its use in life science and biomedical fields, such as wound dressing, coating material, and also for food packing applications.

## FUNDING

The authors are grateful to the Ministry of Education, Youth and Sports of the Czech Republic - NPU Program I (LO1504) and Slovak Grant Agency VEGA for the financial support in the project 2/0156/15. Authors are also thankful to Department of Material Science and Nanotechnology (IISc) Bangalore, India, for TEM analysis.

## REFERENCES

- [1] Regiel, A.; Kyzioł, A. and Arruebo, M.; *Chemik* 67, 683 (2013).
- [2] Dananjaya, S. H. S.; Kulatunga, D. C. M.; Godahewa, G. I.; Lee, J. and Zoysa, M. D.; *RSC Adv.* 6, 33455 (2016).
- [3] Choudhari, S. K.; Kittur, A. A.; Kulkarni, S. S. and Kariduraganavar, M. Y. J.; *Membr. Sci.* 302, 197 (2007).
- [4] Welsh, E. R.; Schauer, C. L.; Qadri, S. B. and Price, R. R.; *Biomacromolecules* 3, 1370 (2002).
- [5] Rani, M.; Agarwal, A. and Negi, Y. S.; *BioResources* 5, 2765 (2010).
- [6] Kumar, S.; Dutta, P. K. and Koh, J.; *Int J Biol Macromol.* 49, 356 (2011).
- [7] Krishnan, S. K.; Prokhorov, E.; Iturriaga, M. H.; Mota-Morales, J. D.; Vázquez-Lepe, M.; Kovalenko, Y.; Sanchez, I. C. and Luna-Bárcenas, G.; *Eur. Polym. J.* 67, 242 (2015).
- [8] Latif, U.; Al-Rubeaan, K. and Saeb, A. T. M.; *International Journal of Polymeric Materials and Polymeric Biomaterials* 64, 448 (2015).
- [9] Govindan, S.; Nivetha, E. A. K.; Saravanan, R.; Narayanan, V. and Stephen, A.; *Appl Nanosci.* 2, 299 (2012).

- [10] Arjunan, N.; Kumari, H. L. J.; Singaravelu, C. M.; Kandalama, R. and Kandasamy, J.; *Int J Biol Macromol.* 2, 77 (2016).
- [11] Durán, N.; Nakazato, G. and Seabra, A. B.; *Appl Microbiol Biotechnol.* 100, 6555 (2016).
- [12] Raza, M. A.; Kanwal, Z.; Rauf, A.; Sabri, A. N.; Riaz, S. and Naseem, S.; *Nanomaterials* 6, 1 (2016).
- [13] Reddy, P. R.; Ganesh, S. D.; Saha, N.; Zandraa, O. and Sáha, P.; *Journal of Nanotechnology* 2016, 1 (2016).
- [14] Pulit-Prociak, J. and Banach, M.; *Open Chem.* 14, 1476 (2016).
- [15] El Din, S. N.; El-Tayeb, T. A.; Abou-Aisha, K. and El-Azizi, M.; *Int J Nanomedicine* 11, 1749 (2016).
- [16] Ganesh, S. D.; Reddy, P. R.; Saha, N. and Saha, P.; *NANOCON-2016, BRNO, Conference paper accepted.*
- [17] Rodkate, N.; Wichai, U.; Boontha, B. and Rutnakornpituk, M.; *Carbohydr. Polym.* 81, 617 (2010).
- [18] Araki, J.; Yamanaka, Y. and Ohkawa, K.; *Polym. J.* 44, 713 (2012).
- [19] Campos, M. G. N.; Satsangi, N.; Rawls, H. R. and Mei, L. H. I.; *ICAM2009, 11<sup>th</sup> International Conference on Advance Material, Brazil, (2009).*
- [20] Krishna Rao, K. S. V.; Ramasubba Reddy, P.; Lee, Y. I. and Kim, C.; *Carbohydr. Polym.* 87, 920 (2012).
- [21] Gan, J. K.; Lim, Y. S.; Huang, N. M. and Lim, H. N.; *RSC Adv.* 6, 88925 (2016).
- [22] Nair, S. B.; Alummoottil, J. N. and Moothandasserry, S. S.; *Starch* 68, 1 (2016).

[23] Azad, A. K.; Sermsintham, N.; Chandkrachang, S. and Stevens, W. F.; J Biomed Mater Res B Appl Biomater. 69, 216 (2004).

[24] Tripathi, S.; Mehrotra, G.K.; and Dutta, P.K.; Bull. Mater. Sci. 34, 29 (2011).

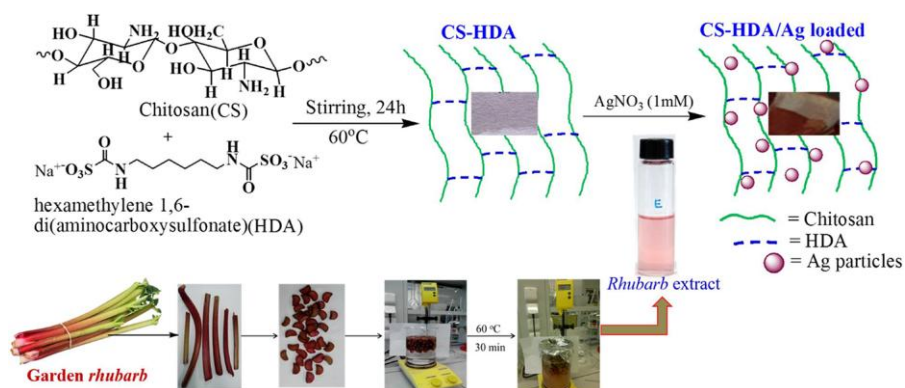
Accepted Manuscript

**Table.1.** Composition of Chitosan based films and their swelling as well as mechanical properties.

Sample Index	Chitosan (4%) ml	HDA (wt%)	ESR (%)	Thickness ( $\mu\text{m}$ )	Mechanical Properties		
					Elongation at break (%)	Tensile strength (MPa)	Young's Modulus (MPa)
CS	100	0	0	82	22.1	24.44	665.86
CS-HDA1	100	2.5	56.12	82	15.7	48.06	1197.35
CS-HDA2	100	5.0	45.70	80	11.9	35.89	1195.53
CS-HDA3	100	7.5	36.52	76	10.3	27.50	1094.01

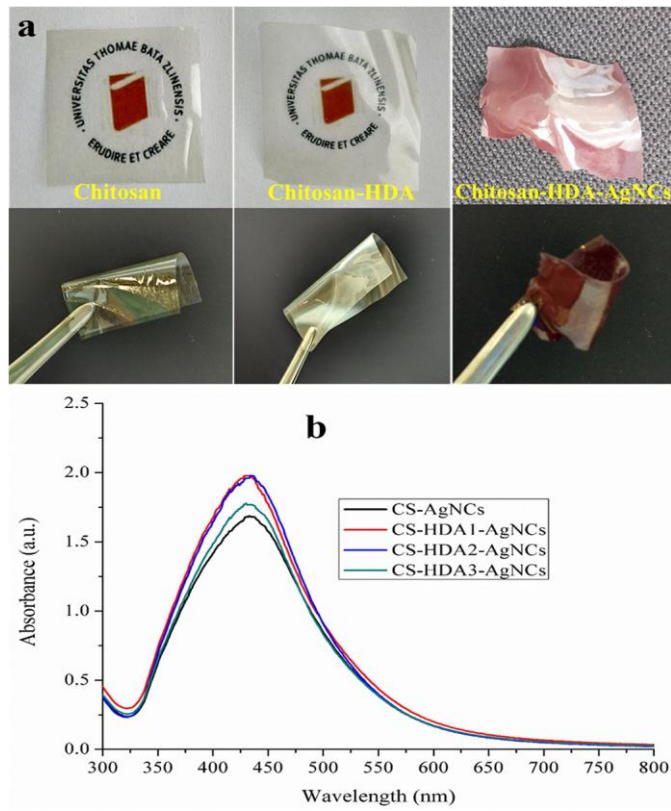


**Scheme 1.** Pictorial illustration of green synthesis of chitosan silver nanocomposite (CS-HDA-AgNCs) films: a novel biomaterial.



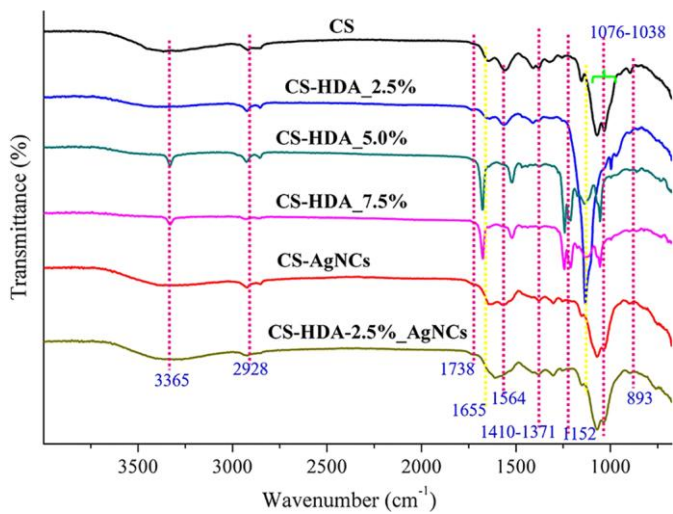
Accepted Manuscript

**Fig.1.** (a) Optical image of CS, CS-HDA & CS-HDA-AgNCs films. (b) UV-vis absorption spectra of CS-AgNCs and CS-HDA-AgNPs.



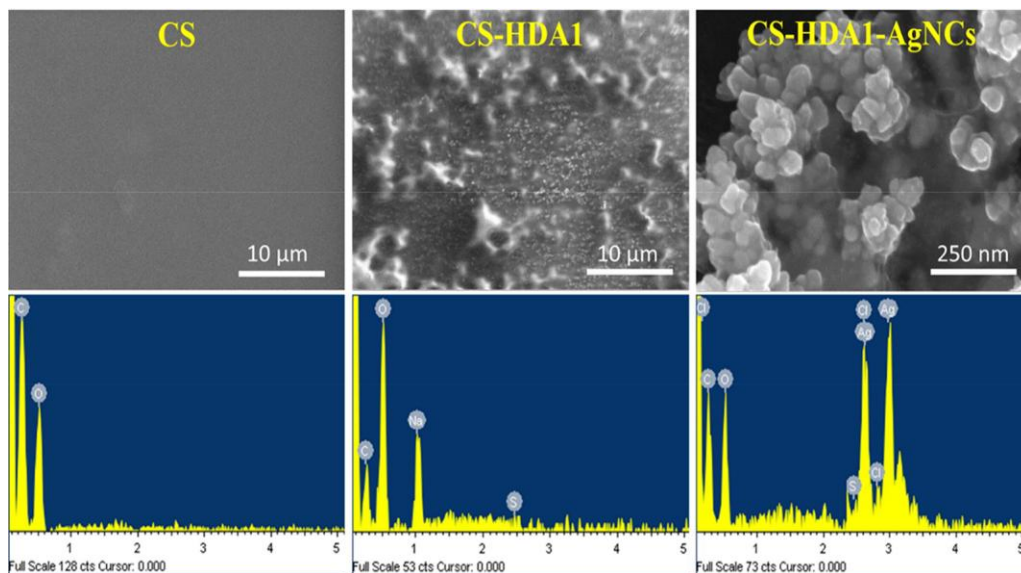
Accepted

**Fig. 2.** FTIR spectra of pure CS, CS-HDA and CS-HDA-AgNCs based biomaterial.



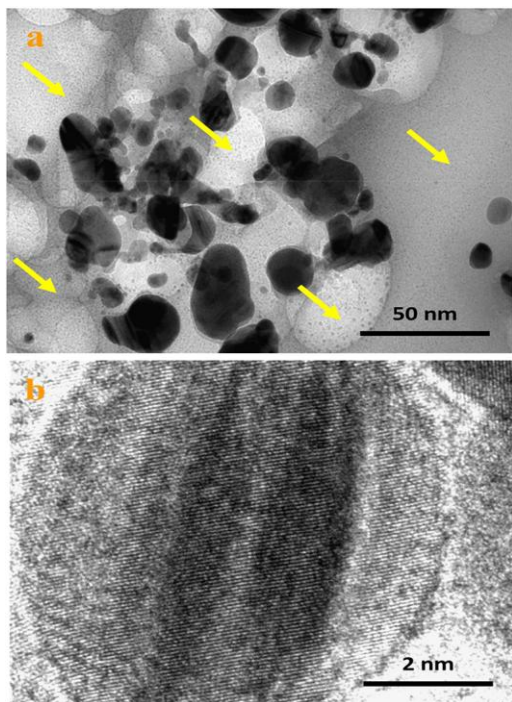
Accepted Manuscript

**Fig. 3.** SEM and EDS analysis of pure CS, CS-HDA1, and CS-HDA1-AgNCs.



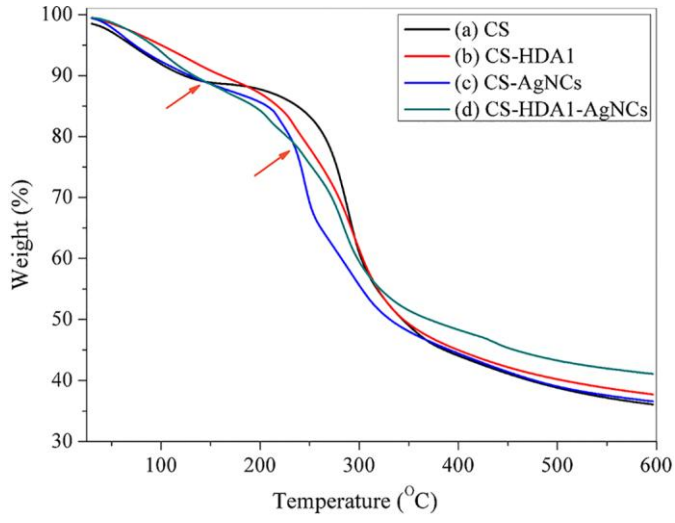
Accepted Manuscript

**Fig. 4.** TEM images of chitosan silver nanocomposites (a) 50nm and (b) 2nm.



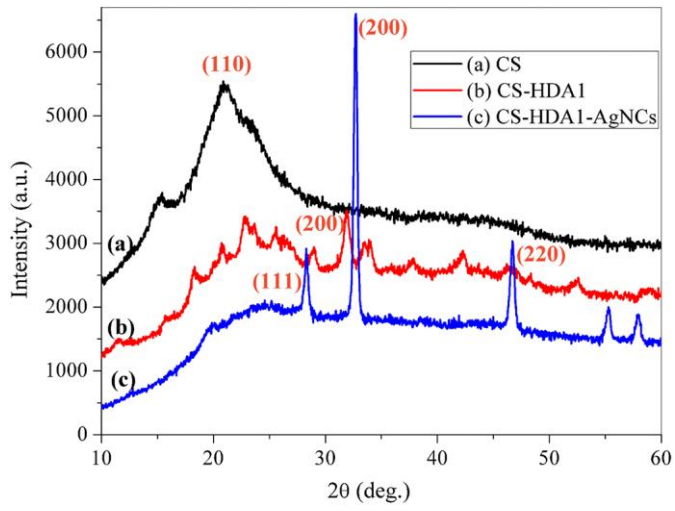
Accepted Manuscript

**Fig. 5.** TGA analysis of (a) CS, (b) CS-HDA1 and (c, d) silver loaded CS, CS-HDA1.



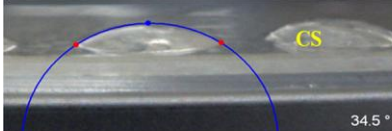
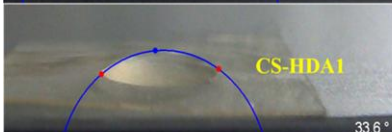
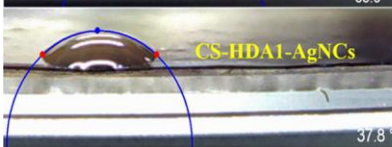
Accepted Manuscript

**Fig. 6.** X-ray diffraction patterns of (a) pure CS, (b) crosslinked CS-HDA1 and (c) CS-HDA1-AgNCs.



Accepted Manuscript

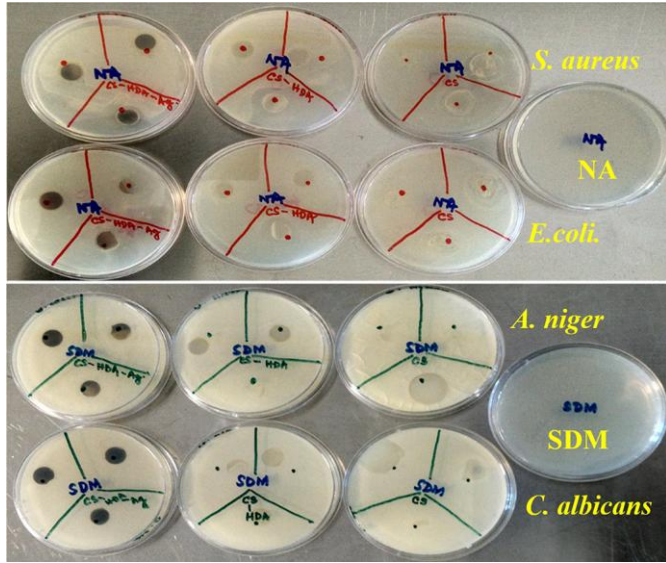
**Fig.7.** Water contact angle measurement of chitosan based films.

Sample Index	Water Contact Angle (°)	Surface energy values (mJ/m <sup>2</sup> )
 CS 34.5°	34.5 ± 4.37	51.52
 CS-HDA1 33.6°	33.6 ± 6.23	62.70
 CS-HDA1-AgNCs 37.8°	37.80 ± 5.26	60.53

Accepted Manuscript

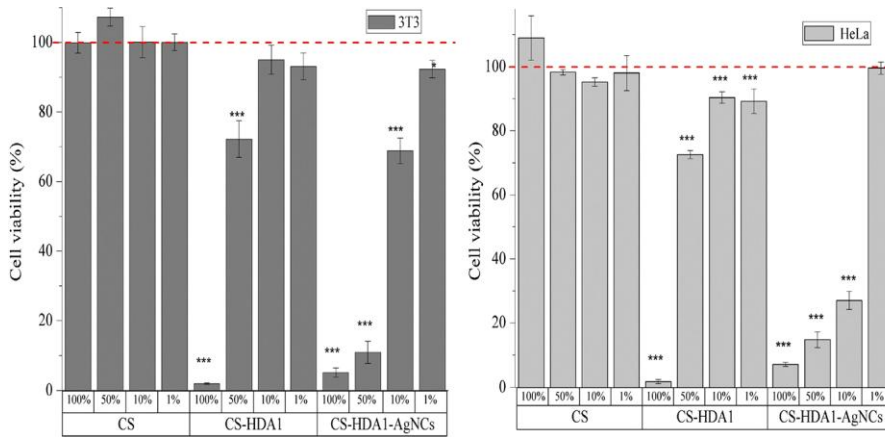


**Fig. 8.** Antimicrobial property of chitosan based biopolymer films



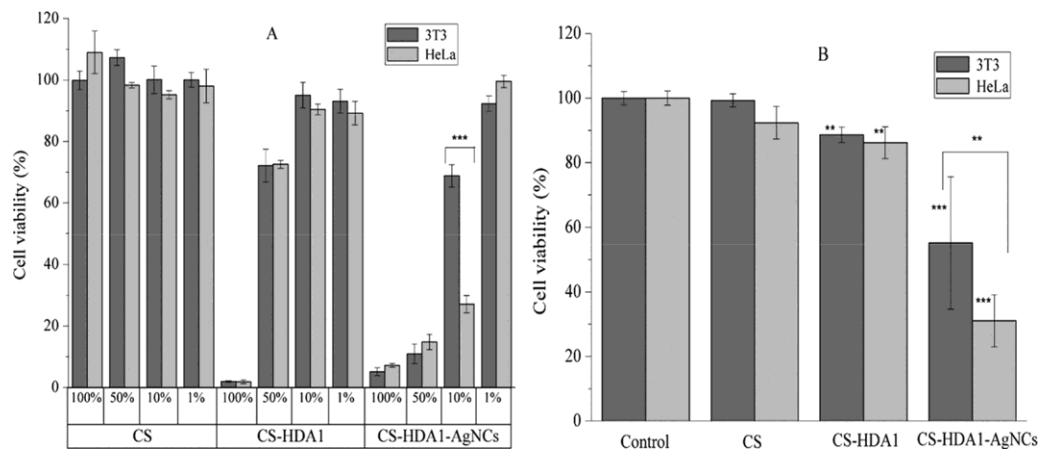
Accepted Manuscript

**Fig. 9.** Cell viability of 3T3 fibroblasts and HeLa cells treated with nanocomposite films extracts to full growth medium. Extracts (100%) and their dilutions (50%, 10% and 1%) were incubated with cells for 24 h. The cell viability is presented as Mean  $\pm$  SD (n=4) compared to untreated control cells corresponding to 100% viability and is shown by red dashed line. The statistical significance is shown by asterisks (\* P < 0.05, \*\* P < 0.05 - 0.01, \*\*\* P < 0.001).



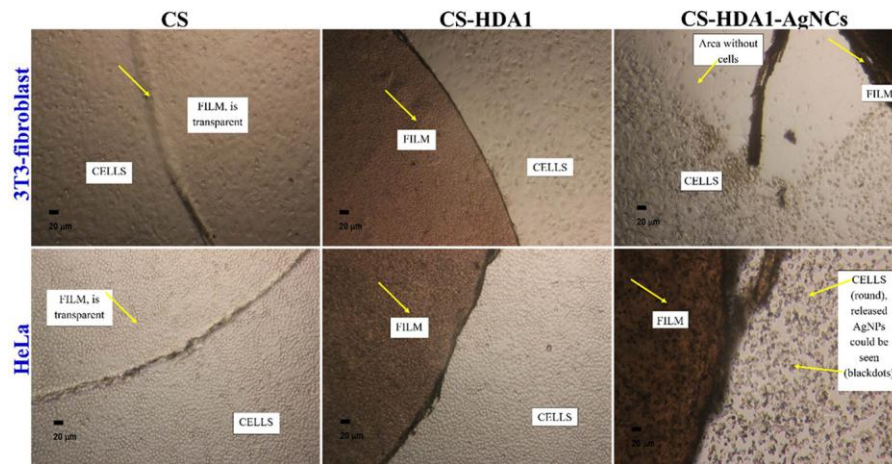
Accepted

**Fig. 10.** Comparison of cell viability between normal 3T3 fibroblasts and cancer HeLa cells (A) Silver nanocomposite films extracts and their dilutions (50%, 10% and 1%). Statistically significant difference between the two cell lines is shown by \*\*\* at  $P < 0.001$ . (B) Direct contact with nanocomposite films. Statistically significant difference between control and the films of each cells type is shown by asterisk next to the bar and statistical difference between the 3T3 and HeLa cells is shown by asterisk above the brackets (\*\*  $P < 0.05 - 0.01$ ), \*\*\*  $P < 0.001$ ).



Accepted

**Fig. 11.** Cytotoxicity assay of surface morphology of (direct contact) chitosan based films.



Accepted Manuscript